# Lamb dip studies of the nuclear quadrupole coupling and dipole moment in an excited vibrational state of $NH_2D$

E. W. Van Stryland and R. L. Shoemaker

*Optical Sciences Center, University of Arizona, Tucson, Arizona 85721*
(Received 19 February 1976)

The hyperfine structure of two transitions in the $\nu_2 = 0 \rightarrow 1$ vibrational band of the asymmetric rotor $NH_2D$ is resolved. These spectra represent the first direct observation of $N^{14}$ nuclear quadrupole splittings in the optical region. The transitions were observed using Lamb dip spectroscopy in which a Stark field is used to tune the spectral components through resonance with a $CO_2$ laser. Splittings of less than 1 MHz are resolved, and the nuclear quadrupole coupling constants in the excited vibrational state are determined to be $\chi_{aa} = 2.52 \pm 0.24$, $\chi_{bb} = 1.46 \pm 0.36$, $\chi_{cc} = -3.98 \pm 0.29$ MHz. In addition, we find $\mu_c = 1.09 \pm 0.04$ D for the excited state permanent dipole moment. These values differ significantly from the ground state values, and some discussion of their physical implications is presented.

## I. INTRODUCTION

Lamb dip spectroscopy is a very powerful tool for obtaining high resolution molecular spectra in the optical region. Small interactions which have been accessible only in ground state molecules using microwave spectroscopy can now be resolved in excited states as well. We report here the first direct observations of $^{14}N$ nuclear quadrupole coupling in the optical region. From the spectra, nuclear quadrupole coupling constants are obtained for an excited vibrational state. In addition, since an electric field is used to tune the spectral components into resonance with the laser, excited state Stark splittings are also observed and an accurate value for the excited state permanent dipole moment obtained.

Our measurements were made on two transitions in the $\nu_2 = 0 \rightarrow 1$ vibrational band of the deuterated ammonia $NH_2D$. One of these transitions has been previously studied using Lamb dip spectroscopy, but the resolution in that work was insufficient to resolve hyperfine structure.[1] A later study using quantum beat spectroscopy provides a measurement of one hyperfine splitting, but this data is insufficient to determine any molecular constants.[2] Here, as many as six components in a single transition are resolved and linewidths (FWHM) as small as 700 kHz obtained.

## II. EXPERIMENTAL

Our experiments were performed using a 1.5 m grating controlled $CO_2$ laser which produces 2–4 W of linearly polarized $TEM_{00}$ radiation on any one of ~50 $CO_2$ lines. A small 650 Hz dither is applied to a piezoelectric on the output mirror and the resulting variation in discharge tube impedance is used to lock the laser to the peak of its gain curve.[3] The long term frequency stability is ~1 MHz, with a short term acoustic jitter of less than 50 kHz. The sample cell is equipped with NaCl windows and contains two $4 \times 30$ cm stainless steel plates separated by six identical $0.889 \pm 0.001$ cm fused quartz spacers. The inner surface of each plate is optically polished and flat to within 0.0003 cm, insuring an extremely uniform electric field between the plates.

After passing through a 20% transmission beam splitter to reduce its intensity, the $CO_2$ laser beam passes through the Stark cell which contains ~3 mTorr $NH_2D$ and is reflected back on itself by a 100% mirror. The experimental arrangement is shown schematically in Fig. 1. Most of the returning beam is reflected off the beamsplitter and focused onto a Honeywell HgCdTe photodiode. A very slight misalignment (~2 mrad) of the return beam combined with a 3 mm aperture at the $CO_2$ laser is sufficient to prevent feedback into the laser cavity.

To observe a Lamb dip, the molecular resonance frequencies were tuned through resonance with the fixed frequency $CO_2$ laser by varying the electric field between the Stark plates. For rough tuning an adjustable dc bais voltage is applied to one Stark plate using a stable high voltage power supply. A linear ramp voltage whose amplitude is adjustable from 0 to 400 V is then applied to the other Stark plate to scan through a resonance. To detect an absorption, the Stark field is modulated by a small (~0.5 V amplitude) 60 kHz square wave which is capacitively coupled to one Stark plate as shown in Fig. 1. The detector output is amplified using a TIXL 151 transimpedance amplifier followed by a PAR CR 4 low noise preamp and a lock-in amplifier. The lock-in output is then fed to an $X$–$Y$ recorder whose $X$ axis is driven by the linear ramp voltage.

The $NH_2D$ was synthesized from $NH_3$ and $D_2O$ and

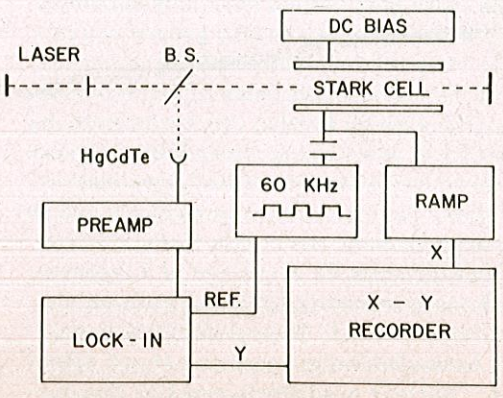


FIG. 1. Experimental arrangement.

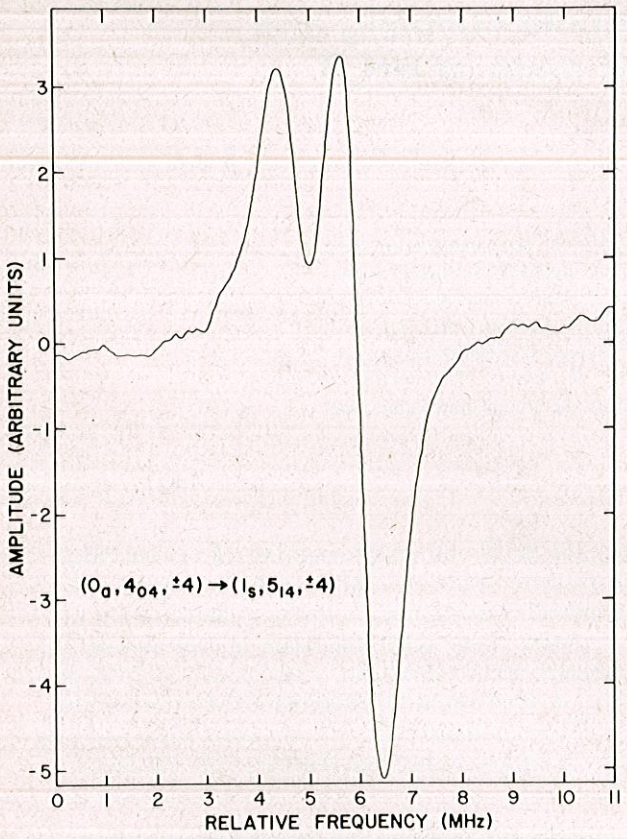


FIG. 2. Observed Lamb dip signal for the $(\nu_2, J, M_J) = (0_a, 4_{04}, \pm 4) \rightarrow (1_s, 5_{14}, \pm 4)$ transition in $NH_2D$.

purified by vacuum distillation. The resulting isotopic mixture of deuterated ammonias contains ~45% $NH_2D$.[4]

## III. RESULTS

Our measurements were made on two transitions in the $\nu_2 = 0 \rightarrow 1$ vibrational band of $NH_2D$, where the $\nu_2$ vibration involves the same normal coordinate as the inversion motion. Because of the inversion, the $\nu_2 = 0$ and 1 vibrational states are split with the components being denoted by a subscript $a$ or $s$ according to whether the wavefunction is antisymmetric or symmetric under inversion.

One set of observations was made on the $(\nu_2, J) = (0_a, 4_{04}) \rightarrow (1_s, 5_{14})$ transition which can be Stark tuned ~2300 MHz into resonance with the $P(14)$ $CO_2$ laser line at 10.53 $\mu$m.[5] The large Stark effect here arises from a near degeneracy between the $4_{04}$ and $4_{14}$ ground states so that the lower state $M_J$ levels are split by several hundred MHz. Thus, in a single Lamb dip trace we observe only transitions which involve one lower state $M_J$ value. A trace with $M_J = \pm 4$ in the lower level is shown in Fig. 2. Since we use a small frequency modulation to detect absorption, first derivative line shapes are observed. In the experiments, the $X$ axis in Fig. 2 is a voltage sweep, but this may be converted to a frequency scale using the lower state Stark tuning rate which is $0.580 \pm 0.006$ MHz/V/cm.[6] The optical field is polarized parallel to the Stark field so that $\Delta M_J = 0$ selection rules apply. Nuclear quadrupole coupling due to the $^{14}N$ nucleus is present here, but for this transition the Stark effect in both the upper and lower states is much larger than the quadrupole coupling. Thus, the $^{14}N$ nucleus is uncoupled from the molecular rotation in both states, resulting in $\Delta M_I = 0$ selection rules and a simple spectrum with two components corresponding to $(M_I, M_J) = (0, \pm 4) \rightarrow (0, \pm 4)$ and $(\pm 1, \pm 4) \rightarrow (\pm 1, \pm 4)$.

A value of $1.24 \pm 0.06$ MHz was obtained for this splitting. We also observed this spectrum with $\Delta M_J = \pm 1$ selection rules. Only two components corresponding to $(0, \pm 4) \rightarrow (0, \pm 5)$ and $(\pm 1, \pm 4) \rightarrow (\pm 1, \pm 5)$ are seen here also since the $\Delta M_J = -1$ components are too weak to be observable. We find a splitting of $0.95 \pm 0.06$ MHz for this transition. The major portion of this is due to the lower state. Fortunately, the lower state splitting can be calculated very accurately since the ground state nuclear quadrupole coupling constants are known from molecular beam work.[7] Thus, the upper state splittings can be extracted and we find

$$\chi_{zz} = eQ\langle \partial^2 V/\partial Z^2 \rangle_{av} = -0.55 \pm 0.08 \text{ MHz} \quad (1)$$

from the standard expression for the matrix elements of the quadrupole operator in an uncoupled basis.[8]

A second set of measurements was made on the $(\nu_2, J) = (0_a, 4_{04}) \rightarrow (1_a, 5_{05})$ transition which can be tuned ~1700 MHz into resonance with the $P(20)$ $CO_2$ laser line at 10.59 $\mu$m.[1,5] For this transition the Stark and quadrupole energies in the upper state are comparable so that we have an intermediate field case. This means a secular equation must be solved to find the energy levels, and a rather complicated spectrum can result since the uncoupled basis selection rules are now partially relaxed.[9] The only rigorous selection rule is $\Delta M = 0, \pm 1$ where $M = M_I + M_J$, although transitions with $\Delta M_I = 0$ still remain the strongest. A trace for which $M_J = \pm 3$ in the lower state and the laser was polarized perpendicular to the Stark field so that $\Delta M = \pm 1$ is shown in Fig. 3. The theoretical spectrum is also shown there with relative intensities proportional to the transition dipole matrix element as this appears to be what is observed. This point is discussed further in Sec. IV.

By rotating the laser polarization 90°, we observed this same transition with $\Delta M = 0$ selection rules. By lowering the bias voltage we also made measurements on components of the $(0_a, 4_{04}) \rightarrow (1_a, 5_{05})$ transition having $M_J = \pm 4$ in the lower state using both $\Delta M = 0$ and $\Delta M = \pm 1$ selection rules. In the course of these measurements we were able to determine the frequency shift between central lines in the $\Delta M = 0$ and $\Delta M = \pm 1$ runs by making alternate scans with different laser polarizations. Taken together, all the data yield a total of 11 observed splittings. We also know that the splitting between the $(M_I, M_J) = (\mp 1, \pm 4)$ and $(\mp 1, \pm 5)$ upper state levels is $1.82 \pm 0.35$ MHz from a previous quantum beat measurement.[2,10] These data are summarized in Tables I and II. A least squares fit of the data is also shown there. The adjustable parameters are the excited state nuclear quadrupole coupling constant and Stark coefficient. We find

$$\chi_{zz} = -2.20 \pm 0.15 \text{ MHz}, \quad (2)$$
$$\Delta E_{\text{Stark}}(5_{05}, M_J) = (1.51 \pm 0.10) \times 10^{-8} M_J^2 \text{ MHz/V}^2/\text{cm}^2 .$$

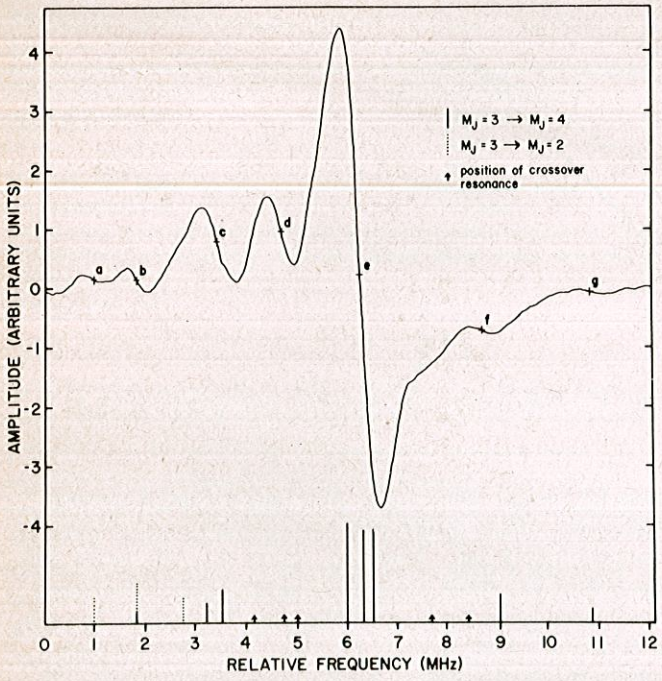


FIG. 3. Observed Lamb dip signal for the $(\nu_2, J) = (0_a, 4_{04}) \rightarrow (1_a, 5_{05})$ transition in $NH_2D$ with $\Delta M = \pm 1$ selection rules and $M_J = \pm 3$ in the lower state. The calculated spectrum is shown along the bottom with possible crossover resonance positions indicated by arrows.

A few of the observed splittings involving averages of two or more transitions may be influenced to some degree by the presence of crossover resonances.[11] To insure that this did not bias our results we also did a least squares fit using only data containing no such ambiguities. The results one obtains are identical.

TABLE I. Observed Lamb dip transitions.

| Label | Transition |
|---|---|
| a | $(0, \pm 3) \rightarrow (0, \pm 2)$ |
| b[a] | $(\pm 1, \pm 3) \rightarrow (\pm 1, \pm 2)$; $(\mp 1, \pm 3) \rightarrow (\pm 1, \pm 2)$ |
| c[a] | $(0, \pm 3) \rightarrow (\pm 1, \pm 3)$; $(\mp 1, \pm 3) \rightarrow (0, \pm 3)$ |
| d | crossover resonances (not used as data). |
| e[a] | $(\pm 1, \pm 3) \rightarrow (\pm 1, \pm 4)$; $(0, \pm 3) \rightarrow (0, \pm 4)$; $(\mp 1, \pm 3) \rightarrow (\mp 1, \pm 4)$ |
| f | $(0, \pm 3) \rightarrow (\mp 1, \pm 5)$ |
| g | $(\pm 1, \pm 3) \rightarrow (0, \pm 5)$ |
| h[a] | $(0, \pm 3) \rightarrow (0, \pm 3)$; $(\pm 1, \pm 3) \rightarrow (\pm 1, \pm 3)$; $(\mp 1, \pm 3) \rightarrow (\mp 1, \pm 3)$ |
| i[a] | $(0, \pm 3) \rightarrow (\mp 1, \pm 4)$; $(\pm 1, \pm 3) \rightarrow (0, \pm 4)$ |
| j[a] | $(\mp 1, \pm 3) \rightarrow (0, \pm 2)$; $(0, \pm 3) \rightarrow (\pm 1, \pm 2)$ |
| k | $(\pm 1, \pm 4) \rightarrow (\pm 1, \pm 4)$ |
| l[a] | $(0, \pm 4) \rightarrow (\mp 1, \pm 5)$; $(\mp 1, \pm 4) \rightarrow (\mp 1, \pm 4)$ |
| m | $(0, \pm 4) \rightarrow (0, \pm 4)$ |
| n | $(\mp 1, \pm 4) \rightarrow (0, \pm 4)$ |
| o[a] | $(\pm 1, \pm 4) \rightarrow (\pm 1, \pm 5)$; $(0, \pm 4) \rightarrow (0, \pm 5)$; $(\mp 1, \pm 4) \rightarrow (\mp 1, \pm 5)$ |
| p | $(\mp 1, \pm 4) \rightarrow (\mp 1, \pm 5)$ taken from Ref. 2. |

All transition are $(\nu_2, J) = (0_a, 4_{04}) \rightarrow (1_a, 5_{05})$ and are labeled in the uncoupled basis $(M_I, M_J)$ where a through g correspond to the labeling of Fig. 3.

[a]Unresolved transitions.

TABLE II. Observed splittings.

| Splitting | | Observed (MHz) | Calculated (MHz) | Difference |
|---|---|---|---|---|
| a | b | 0.93 ± 0.07 | 0.84 | 0.09 |
| b | e | 4.28 ± 0.10 | 4.20 | 0.08 |
| c | e | 2.66 ± 0.13 | 2.72 | −0.06 |
| e | f | 2.53 ± 0.15 | 2.61 | −0.08 |
| e | g | 4.45 ± 0.21 | 4.40 | 0.05 |
| h | i | 2.57 ± 0.23 | 2.55 | 0.02 |
| j | h | 2.21 ± 0.10 | 2.18 | 0.03 |
| k | l | 0.96 ± 0.03 | 0.92 | 0.04 |
| m | k | 0.89 ± 0.03 | 0.89 | 0.00 |
| n | o | 1.48 ± 0.03 | 1.47 | 0.01 |
| k | o | 1.75 ± 0.16 | 1.94 | −0.19 |
| n | p | 1.82 ± 0.35 | 1.79 | 0.03 |

As measured between transitions shown in Table I. Average frequencies for unresolved transitions are calculated using a weighted average according to the relative dipole matrix elements.

The nuclear quadrupole coupling constants in Eqs. (1) and (2) are proportional to the average values of the electric field gradient at the $^{14}N$ nucleus along a space fixed axis. These numbers may be combined to yield the field gradients along three principal axes fixed in the molecule by means of the relation[12]

$$\left\langle \frac{\partial^2 V}{\partial Z^2} \right\rangle_{av} = \frac{2}{(J+1)(2J+3)} \sum_g \langle J_\tau | P_g^2 | J_\tau \rangle \left( \frac{\partial^2 V}{\partial g^2} \right) \tag{3}$$

together with the Laplace equation

$$\frac{\partial^2 V}{\partial a^2} + \frac{\partial^2 V}{\partial b^2} + \frac{\partial^2 V}{\partial c^2} = 0 \, . \tag{4}$$

Here $g$ is one of the principal axes $a$, $b$, or $c$, $\langle \partial^2 V / \partial Z^2 \rangle_{av}$ is the average field gradient along a space fixed axis for the rotational state $J_\tau$, and $\langle J_\tau | P_g^2 | J_\tau \rangle$ is the average value of the square of the angular momentum along the $g$th principal axis in that state.

To use Eq. (3) we must know the matrix elements $\langle J_\tau | P_g^2 | J_\tau \rangle$. These depend on the molecular structure in the excited vibrational state, in particular, on the asymmetry parameter $\kappa = (2B - A - C)/(A - C)$. While an accurate excited state $\kappa$ is not known for $NH_2D$, one does not expect it to change dramatically from its ground state value of $\kappa = -0.310$.[13] Rotational constants are known for the $\nu_2 = 1$ excited vibrational state in both $NH_3$ and $ND_3$ so that excited state structures can be calculated for both of these molecules.[14] The results show that the bond lengths and angles increase by approximately 0.005 Å and 1° in $NH_3$ with similar changes for $ND_3$. To estimate the range over which $\kappa$ might vary in $NH_2D$, we doubled these changes and assumed a worst case situation in which the N–H bond lengths and angles increase while the N–D bond remains essentially unchanged (allowing the N–D bond to change also, gives a $\kappa$ which differs little from the ground state value). These calculations show that it is possible, though not likely, for $\kappa$ to change from its ground state value to a value as low as −0.25.

Using the ground state $\kappa$ in Eqs. (3) and (4) we find

$$eQ(\partial^2 V/\partial a^2) = 2.52 \pm 0.24 \text{ MHz},$$
$$eQ(\partial^2 V/\partial b^2) = 1.46 \pm 0.36 \text{ MHz}, \quad (5)$$
$$eQ(\partial^2 V/\partial c^2) = -3.98 \pm 0.29 \text{ MHz}.$$

The error limits here are determined by the experimental errors in determining $eQ\langle\partial^2 V/\partial Z^2\rangle_{av}$. When $\kappa = -0.25$ is used in Eqs. (3) and (4), the results change only slightly with $\partial^2 V/\partial a^2$ and $\partial^2 V/\partial b^2$ becoming more nearly equal and $\partial^2 V/\partial c^2$ remaining unchanged. However, all values remain within the error limits shown in Eqs. (5). Thus, provided our assumptions about the $NH_2D$ structural changes are correct, Eqs. (5) provide the nuclear quadrupole coupling constants even though an exact excited state value of $\kappa$ is not known.

The Stark coefficient for the $\nu_2 = 1$, $J = 5_{05}$ level given in Eq. (2) yields a value for the $NH_2D$ excited state permanent dipole moment. This may be obtained from the standard second order perturbation theory expression[15]

$$\Delta E_{\text{Stark}}(J_\tau, M_J) = \sum_g \mu_g^2 \epsilon^2 \sum_{J'_\tau, M'_J} \frac{|\langle J_\tau M_J | \phi_{Zg} | J'_\tau M'_J \rangle|^2}{E_{J_\tau} - E_{J'_\tau}} . \quad (6)$$

Here $\epsilon$ is the applied Stark field, $\phi_{Zg}$ is a direction cosine, and $\mu_g = \langle \psi_{el}\psi_{vib}\psi_{inv} | \sum_i e_i g_i | \psi_{el}\psi_{vib}\psi'_{inv}\rangle$ with $g_i$ being the $g$ coordinate of the $i$th electron or nucleus in the molecule. If $\psi_{inv}$ is the antisymmetric inversion state then $\psi'_{inv}$ is the symmetric state and vice versa. $\mu_g$ is thus the dipole moment component along the principal axis $g$ as seen by the rotating molecule (i.e., averaged over vibration and inversion).[16] The energy differences $E_{J_\tau} - E_{J'_\tau}$ should be understood to include inversion splittings as well as the rotational energies. In practice, only a few nearby levels contribute significantly to the summation over $J'_\tau$ in Eq. (6) and we obtain

$$\mu_c = 1.09 \pm 0.04 \text{ D}. \quad (7)$$

Note that only $\mu_c$ is obtained here. $\mu_b$ is zero by symmetry and $\mu_a$, which we expect to be small in any event, makes a negligible contribution to $\Delta E_{\text{Stark}}(5_{05}, M_J)$. The reason is that the nearest $a$-dipole connected levels to $5_{05}$ contribute almost equally but with opposite signs, producing a Stark shift for $\mu_a$ which is nearly zero.

To calculate $\mu_c$ one must know the direction cosine matrix elements, which depend on $\kappa$. The ground state value of $\kappa$ was used to obtain Eq. (7), but the $\kappa$ dependence of the relevant matrix elements is very small and the results are unchanged for any $\kappa$ between $-0.25$ and $-0.31$. The energy level differences $E_{J_\tau} - E_{J'_\tau}$ must also be known. Since only $J = 5$ levels contribute significantly, these differences depend on $\kappa$, $A-C$, and the inversion splitting. However, given a $\kappa$, the latter two quantities are fixed since two energy level differences are known from laser spectroscopy.[5,17] Again, for any $\kappa$ between $-0.25$ and $-0.31$, the $\mu_c$ one obtains lies within the experimental error limits shown in Eq. (7).

TABLE III. Nuclear quadrupole coupling constants in the $\nu_2 = 1$ excited vibrational state compared to the ground state constants.

| $NH_2D$ excited state $\nu_2 = 1$ | $NH_2D$ ground state[a] |
|---|---|
| $eQ(\partial^2 V/\partial a^2) = 2.52 \pm 0.24$ MHz | 1.902 MHz |
| $eQ(\partial^2 V/\partial b^2) = 1.46 \pm 0.36$ MHz | 2.042 MHz |
| $eQ(\partial^2 V/\partial c^2) = -3.98 \pm 0.29$ MHz | −3.944 MHz |

[a]From Ref. 18.

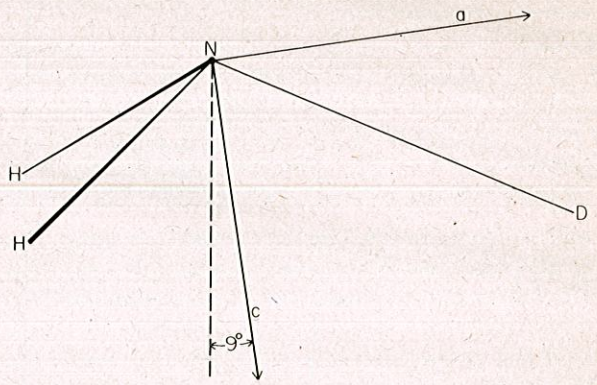


FIG. 4. Orientation of the principal axis system in $NH_2D$.

## IV. DISCUSSION

The Lamb dip relative intensities observed in our experiments are nearly proportional to the transition dipole matrix elements $\mathcal{P}_{ab}$ (c.f. Fig. 3). This is in contrast to standard perturbation theory treatments of the Lamb dip which predict relative intensities that go as $\mathcal{P}_{ab}^4$.[11] However, these theories assume that one beam is weak while experimentally both forward and return beams had high intensity. In fact, the optical field strengths used (~ 50 V/cm) were sufficiently high to significantly broaden the stronger transitions thus reducing their apparent intensity relative to weaker transitions. The effect is enhanced by the fact that we observe the derivative of the absorption line shape. We found high power operation to be desirable since it enabled us to observe several very weak transitions. The tradeoff is some loss in resolution. All attempts to increase the resolution by lowering the power resulted simply in the disappearance of the weak transitions. We note that the crossover resonances are also weaker than predicted by the usual theoretical treatments. This phenomenon has been observed by a number of workers.

Table III shows our results for the nuclear quadrupole coupling constants in the $\nu_2 = 1$ excited vibrational state as compared to the ground state constants which were obtained by Kukolich using molecular beam methods.[18] We note first that the ground state values are exactly what one would expect if the electronic charge distribution in $NH_2D$ were identical to $NH_3$. This may be seen by rotating the $NH_3$ field gradient tensor into the $NH_2D$ principal axis system which is shown in Fig. 4. $NH_3$ has $\chi = -4.092$ MHz along the threefold symmetry axis of the electronic charge distribution (the dotted line in Fig. 4) and quadrupole coupling constants of $-\frac{1}{2}\chi$ along the two perpendicular axes.[19] A 9° rotation of this tensor reproduces the $NH_2D$ quadrupole coupling constants

TABLE IV. Electric dipole moments in $NH_2D$ compared to $NH_3$.

| | |
|---|---|
| $NH_2D$ excited state $\nu_2=1$ | $NH_2D$ ground state[a] |
| $\mu_c=1.09\pm0.04$ D | 1.47 D |
| $NH_3$ excited state $\nu_2=1$[b] | $NH_3$ ground state |
| $\mu=1.25\pm0.01$ D | 1.468 D |

[a]This value is calculated from the Stark tuning rate reported in Refs. 1 and 6.
[b]From Ref. 20.

to very high accuracy (< 1%). In the $\nu_2=1$ state, however, the threefold symmetry of the electronic charge distribution is evidently broken since we now have $\chi_{aa}$ considerably greater than $\chi_{bb}$ and these values cannot be obtained by any reasonable rotation of a quadrupole coupling tensor for a threefold symmetric electronic charge distribution. This is not unexpected since the deuterium nucleus in $NH_2D$ is twice as massive as the H nucleus and thus will have a considerably smaller vibrational amplitude in the $\nu_2=1$ state. It would be interesting to see if the rotational constants for this state also show a breaking of the threefold symmetry of the molecule. Unfortunately, sufficient data to determine them is not presently available.

In Table IV, we show our result for the $\nu_2=1$ state electric dipole moment in $NH_2D$ as compared to electric dipole moment values in $NH_3$. In both molecules the dipole moment in the excited state is much smaller than in the ground state. One is tempted to attribute this to a flattening of the $NH_3$ and $NH_2D$ pyramids, but the small observed structural changes in $NH_3$ on going to the $\nu_2=1$ state indicate that electronic charge redistribution during vibration must be the major factor in reducing $\mu$. The $\nu_2=1$ dipole moment in $NH_2D$ is smaller than in $NH_3$ even though the ground state values are comparable. No simple physical reason for this is evident to us although part of the difference may be due to the fact that we have measured only $\mu_c$ in $NH_2D$ while $\mu_{\text{Total}}=\sqrt{\mu_c^2+\mu_a^2}$. One expects $\mu_a$ to be nonzero due to the breaking of the threefold symmetry of the electronic charge distribution in $\nu_2=1$ as well as the ~9° tilt of the principal axis system (see Fig. 4). It would be interesting to measure $\mu_a$ using other $NH_2D$ transitions.

## ACKNOWLEDGMENT

The support of the National Science Foundation is gratefully acknowledged.

[1]R. G. Brewer, M. J. Kelly, and A. Javan, Phys. Rev. Lett. 23, 559 (1969).
[2]R. L. Shoemaker and F. A. Hopf, Phys. Rev. Lett. 33, 1527 (1974).
[3]W. H. Thomason and D. C. Elbers, Rev. Sci. Instrum. 46, 409 (1975).
[4]R. L. Shoemaker and E. W. Van Stryland, J. Chem. Phys. 64, 1733 (1976).
[5]M. J. Kelly, R. E. Francke, and J. J. Feld, J. Chem. Phys. 53, 2979 (1970).
[6]T. A. Nussmeier and R. L. Abrams, Appl. Phys. Lett. 25, 615 (1974).
[7]S. G. Kukolich, J. Chem. Phys. 49, 5523 (1968).
[8]J. M. B. Kellogg, I. I. Rabi, N. F. Ramsey, Jr., and J. R. Zacharias, Phys. Rev. 57, 677 (1940).
[9]M. Mizushima, J. Chem. Phys. 21, 539 (1953).
[10]This splitting was erroneously listed as 2.4 MHz. in Ref. 2.
[11]See, for example, H. R. Schlossberg and A. Javan, Phys. Rev. 150, 267 (1966).
[12]Equation (3) may be obtained by expanding $\langle \partial^2 V/\partial Z^2\rangle_{av}$ in terms of direction cosine matrix elements and then using Appendix A in W. Huttner and W. H. Flygare, J. Chem. Phys. 47, 4137 (1967).
[13]F. C. DeLucia and P. Helminger, J. Mol. Spectrosc. 54, 200 (1975).
[14]W. S. Benedict and E. K. Plyler, Can. J. Phys. 35, 1235 (1957).
[15]J. E. Wollrab, *Rotational Spectra and Molecular Structure* (Academic, New York, 1967).
[16]M. T. Weiss and M. W. P. Strandberg, Phys. Rev. 83, 567 (1951).
[17]A value for the $NH_2D$ $\nu_2=1$ inversion splitting is given in Ref. 5, but the ground state value of $\kappa$ was assumed in order to obtain this number.
[18]S. G. Kukolich, J. Chem. Phys. 49, 5523 (1968).
[19]S. G. Kukolich and S. C. Wofsy, J. Chem. Phys. 52, 5477 (1970).
[20]F. Shimizu, J. Chem. Phys. 51, 2754 (1969).